Inorganic Chemistry

Article

pubs.acs.org/IC

Symmetrically Related Construction and Optical Properties of Two Noncentrosymmetric 3D Iodides of d^{10} Cation (Cu^+, Ag^+) Based on the *N*-Benzylpyridinium and Its Supramolecular Interactions

Yanrong Qiao, Pengfei Hao, and Yunlong Fu*

School of Chemistry & Material Science, Shanxi Normal University, Linfen 041004, P. R. China

Supporting Information

ABSTRACT: Two noncentrosymmetric compounds, namely, $[N\text{-Bz-Py}]_2[Cu_6I_8]$ (**1**) and $[N\text{-Bz-Py}]_4[Ag_9I_{13}]$ (**2**) (N-Bz-Py$^+$ = N-benzylpyridinium), with three-dimensional open frameworks, were synthesized solvothermally via in situ benzylation of pyridine. **1** is constructed from 3-connected Cu_3I_7 secondary building units (SBUs) with chiral (10,3)-a topology, while the occluded N-Bz-Py$^+$ forms a complementary supramolecular (10,3)-a net via $\pi-\pi$ interactions. **2** is characteristic of acentric connections of trimeric Ag_3I_8 and hexamer Ag_6I_{12} SBU, while N-Bz-Py$^+$ in the channels aggregates into asymmetrically supramolecular chains via $\pi-\pi$ interactions. Remarkable structural correlations imply the unique amplification and transfer of asymmetric information from V-shaped N-Bz-Py$^+$ to organic supramolecular nets and inorganic frameworks, which are confirmed by their second harmonic generation responses. Adsorption spectra reveal their semiconductive nature (2.52 eV for **1** and 3.02 eV for **2**) and interesting reversible thermochromism for **1** based on the intermolecular charge transfer.

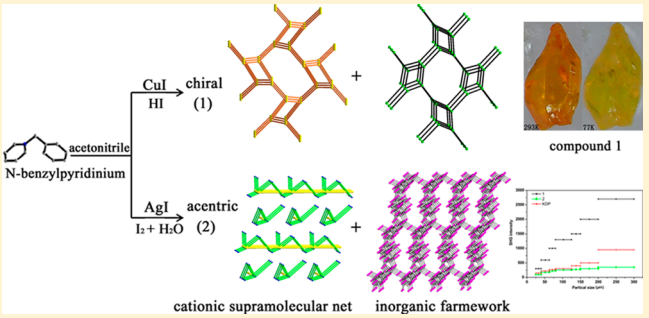

1. INTRODUCTION

Directed synthesis has been widely used as an effective strategy in the construction of functional materials. Noncentrosymmetric (NCS) materials are of current interest and great importance owing to their potential applications, such as second-order nonlinear optics (NLO),[1] pyroelectricity,[2] ferroelectricity,[3] piezoelectric,[4] enantioselective sorption, separation, and catalysis.[5] Despite a lot of progress, rational construction of NCS materials from achiral primary building units (PBUs) is particularly difficult due to their unclear mechanism, especially in the field of organically directed inorganic framework.[6] Generally, the occurrence of NCS inorganic framework depends on three factors, crystallizing habit of inorganic components,[7] spatial and electronic configuration of structure directing agents (SDAs),[8,9] and their interactions.[10] Instinctively, chiral templates are first applied to impart their chirality and facilitate the formation of chiral or acentric framework, which has achieved some success, such as chiral gallophosphates directed by chiral organic amines,[8] metal phosphates,[9] germinates,[11] and borates[12] by chiral metal complexes. Alternatively, some interesting but challenging strategies based on the spontaneous resolution have been noticed, including chiral $[CN_3H_6][Sn_4P_3O_{12}]$[13] and NCS $(NH_4)_2Te_2WO_8$[14] built from the asymmetric SnO_3, TeO_4, and WO_6, as well as chiral $(NH_4)_2[Zn(SO_4)_2]$ and $[Ti_3P_6O_{27}]\cdot 5[NH_3CH_2CH_2NH_3]\cdot 2[H_3O]$, which resulted from low symmetrical linkages of PBU.[15,16] Unfortunately, this kind of spontaneous chiral resolution occurring within inorganic framework is usually difficult to predict. Therefore, it is still a challenge how to rationally construct chiral or acentric framework from achiral inorganic PBUs. SDAs as a crucial factor not only play "space-filling" roles to modulate the complexity and dimensions of inorganic framework[17] but also could exert their asymmetric impact on the resultant framework, suggesting a potential route to the spontaneous chiral resolution of inorganic framework and reasonable design of NCS materials.

The iodides of d^{10} cation (Cu^+, Ag^+) possess flexible μ-I linkage modes, local charge density, metallophillic interactions, and electron-rich feature. These features could display more sensitive response to the spatial and electronic configuration of SDAs and be regarded as an ideal candidate for the structural directing assembly of inorganic framework, in particular chiral or acentric structures with multifunctional properties.

Herein, in situ derived chiral N-Bz-Py$^+$ cation was used as a potential asymmetric source, and Cu/Ag iodides were used as inorganic components to explore the symmetrically directing effect of SDA on the iodocuprate and iodoargentate. Results reveal that supramolecular aggregations of N-Bz-Py$^+$ realize the amplification and transfer of cationic asymmetric information and consequent assembly of chiral $[N\text{-Bz-Py}]_2[Cu_6I_8]$ (**1**) and acentric $[N\text{-Bz-Py}]_4[Ag_9I_{13}]$ (**2**) with second harmonic

Received: June 13, 2015
Published: August 26, 2015

DOI: 10.1021/acs.inorgchem.5b01331
Inorg. Chem. 2015, 54, 8705−8710

generation (SHG) responses. Furthermore, the thermochromic behavior of **1** is also investigated.

2. EXPERIMENTAL SECTION

Preparation of $\{[N\text{-Bz-Py}]_2[Cu_6I_8]\}_n$ (1). A mixture of pyridine (99.5 wt %, 0.051 g, 0.65 mmol), CuI (99 wt %, 0.570 g, 3.0 mmol), and acetonitrile (99 wt %, 3.0 mL) was heated with concentrated HI (0.37 mL, 1.95 mmol, 45%) and benzyl alcohol (98 wt %, 4.0 mL) in a 15 mL Teflon-lined stainless steel vessel for 3 d at 110 °C. The mother liquor was stored at room temperature for 1 d to afford **1** as orange block crystals. The yield was 46.32% yield based on Cu. Chemical analysis indicates the contents of Cu and I as 21.91 and 58.39 wt % (calculated: 21.95 and 58.45 wt %), giving the Cu/I molar ratio of 3:4. Anal. Calcd for $C_{24}H_{24}N_2Cu_6I_8$: C, 16.60; H, 1.39; N, 1.61%. Found: C, 16.62; H, 1.38; N, 1.61%. IR (KBr, cm^{-1}): ν 3039(m), 2924(m), 2845(m), 1632(s), 1486(m), 1453(m), 1390(w), 1259(w), 1207(w), 1160(m), 1060(m), 745(m), 688(m), 562(m).

Preparation of $\{[N\text{-Bz-Py}]_4[Ag_9I_{13}]\}_n$ (2). The procedure was similar to the synthesis of compound **1**, except that AgI (99 wt %, 0.705 g, 3.0 mmol) was used instead of CuI, and concentrated HI was replaced by I_2 (99.8 wt %, 0.495 g, 1.95 mmol) and water (0.05 mL). Pale-yellow block crystals were achieved in 40.83% yield (based on Ag). Chemical analysis indicates the contents of Ag and I as 29.36 and 49.60 wt % (calculated: 29.41 and 49.67 wt %), giving the Ag/I molar ratio of 9:13. Anal. Calcd for $C_{48}H_{48}N_4Ag_9I_{13}$: C, 17.46; H, 1.47; N, 1.70%. Found: C, 17.45; H, 1.47; N, 1.71%. IR (KBr, cm^{-1}): ν 3050(m), 2926(m), 2852(w), 1631(s), 1478(s), 1442(m), 1396(w), 1345(m), 1284(w), 1214(m), 1151(m), 1020(m), 765(s), 679(s), 546(m).

As a green, effective, and economic way,[18,19] in situ alkylation of organic amines has been widely used for the synthesis of iodometallate hybrids. Although $[N\text{-Bz-Py}]^+$ cations were formed in situ with benzyl alcohol as *N*-alkylated reagent, **1** was prepared in the presence of HI acid, pyridine, and benzyl alcohol under solvothermal conditions, while **2** could only be obtained in the presence of iodine and a small amount of water instead of HI acid. The difference of synthetic conditions exhibits distinct effects of inorganic components in the alkylation process.

X-ray Crystallography. Crystallographic data were recorded at 293 K (for **1** and **2**) and 100 K (for **1**) on an Oxford Gemini diffractometer using graphite monochromated Mo Kα (λ = 0.710 73 Å). An empirical absorption correction with spherical harmonics was performed by SCALE3 ABSPACK scaling algorithm.[20] All the three structures were solved by direct methods and refined by full-matrix least-squares techniques on F^2 performed with SHELXTL-97 program.[21] All non-hydrogen atoms were treated anisotropically. The single-crystal data of **1** and **2** are detailedly described in Table 1. Selected bond lengths and bond angles are listed in Table S1 of the Supporting Information.

Materials and Methods. All chemicals used in the synthesis were commercially sourced and used without further purification. X-ray powder diffraction (XRPD) patterns were collected using a Rigaku Ultima IV−185 diffractometer. Elemental analyses (C, H, N) were conducted on a Perkin-Elmer 240 elemental analyzer. Inductively coupled plasma (ICP) analyses were performed on a Perkin-Elmer 2400 Elemental Anal. FT-IR spectra (4000−400 cm^{-1}) were obtained with a Nicolet 5DX spectrometer by use of KBr pellets. UV−vis diffuse reflectance spectrum was performed on a Varian Cary 5000 UV−vis spectrophotometer at room temperature and at 77 K. Thermogravimetric experiments were performed using an HTG-3 equipment in air in the range of 25−920 °C at 10 °C·min^{-1}.

Second Harmonic Generation Measurements. SHG responses were measured on the polycrystalline powder samples of **1** and **2** and estimated by the method of Kurtz and Perry with Q-switched Nd:YAG lasers with λ = 1064 nm.[22] The samples were ground and sieved into several different particle-size ranges of 25−40, 40−63, 63−80, 80−125, 125−150, 150−200, and 200−300 μm. Meanwhile, the potassium dihydrogen phosphate (KDP) powder was sieved into the same particle-size ranges as the reference. Then they were pressed between glass slides and secured with tape in aluminum holders (1 mm thickness) containing a hole (8 mm diameter). The ratio of the SHG effect was obtained based on the density of SHG outputs of **1**, **2**, and KDP with the same particle-size range of 200−300 μm (Figure S1, Supporting Information).

Table 1. Crystal Data and Structure Refinement for Compounds 1 and 2

compound	1		2
CCDC code	1060214	1060213	1060215
temperature	293(2) K	100(2) K	293(2) K
formula	$C_{24}H_{24}N_2Cu_6I_8$	$C_{24}H_{24}N_2Cu_6I_8$	$C_{48}H_{48}N_4Ag_9I_{13}$
formula weight	1736.89	1736.89	3300.43
crystal size (mm)	0.18 × 0.10 × 0.09	0.18 × 0.10 × 0.09	0.17 × 0.11 × 0.09
crystal system	orthorhombic	orthorhombic	monoclinic
space group	$P2_12_12_1$	$P2_12_12_1$	Cc
a (Å)	14.4193(7)	14.2237(5)	22.5616(13)
b (Å)	14.7830(7)	14.7140(4)	15.4537(8)
c (Å)	17.2685(9)	17.1597(4)	21.8953(13)
α (deg)	90	90	90
β (deg)	90	90	111.133(7)
γ (deg)	90	90	90
V (Å^3)	3681.0(3)	3591.29(18)	7120.6(7)
Z	4	4	4
D_c (g cm^{-3})	3.134	3.212	3.079
F (000)	3120	3120	5900
μ (mm^{-1}) Flack parameter	10.133 − 0.04(4)	10.386 0.04(3)	8.089 − 0.04(3)
reflections collected	11 023	10 844	16 004
unique reflections	7049	6424	10 512
Rint	0.0443	0.0316	0.0284
goodness-of-fit on F^2	1.001	1.047	1.039
$R1/wR2$, $[I \geq 2\sigma_I]^{a,b}$	0.0415, 0.0769	0.0310, 0.0608	0.0425, 0.0993
$R1/wR2$ (all data)	0.0477, 0.0816	0.0354, 0.0628	0.0519, 0.1076
$\Delta\rho_{max}$, $\Delta\rho_{min}$ (e Å^{-3})	1.851, −1.356	0.974, −1.146	3.221, −1.216

$^aR_1 = \sum||F_0| - |F_c||/\sum|F_0|$. $^bwR_2 = [\sum w(F_0^2 - F_c^2)^2/\sum w(F_0^2)^2]^{1/2}$.

3. RESULTS AND DISCUSSION

3.1. Infrared Spectral Aspects. The IR spectra of **1** and **2** (Figure S2) show similar features due to the existence of *N*-Bz-Py$^+$ cations. The medium bands at ∼2930 cm^{-1} are assigned to C−H stretching vibrations of methylene groups, while those at 3040 cm^{-1} (m) to C−H stretching vibrations of aromatic rings; strong or medium peaks at ∼1630, 1480, 1450, and 1060 cm^{-1} could indicate the presence of pyridyl or benzene group.[23]

3.2. Description of Structures. *$\{[N\text{-Bz-Py}]_2[Cu_6I_8]\}_n$ (1).* Compound **1** crystallizes in chiral space group $P2_12_12_1$ with a Flack parameter of −0.04(4), revealing an enantiopure crystal although its bulk product may be racemic. The asymmetric unit of compound **1** contains six Cu(I) atoms and eight iodine atoms together with two *N*-Bz-Py$^+$ cations (Figure 1). Each Cu atom is coordinated by four μ_3-I atoms to form a distorted tetrahedral geometry. The Cu−I bond distances range from 2.6345(19) to 2.7430(16) Å, and I−Cu−I bond angles vary between 99.24(5)° and 117.74(7)°, deviating slightly from an ideal tetrahedron. Cu···Cu distances are 2.733(2)−2.917(2) Å, among which the remarkably short contacts for Cu(2)−Cu(3) (2.733(2) Å) and Cu(2)−Cu(6) (2.749(2) Å) are less than twice the van der Waals radius (1.4 Å) of Cu(I), implying Cu−

DOI: 10.1021/acs.inorgchem.5b01331
Inorg. Chem. 2015, 54, 8705−8710

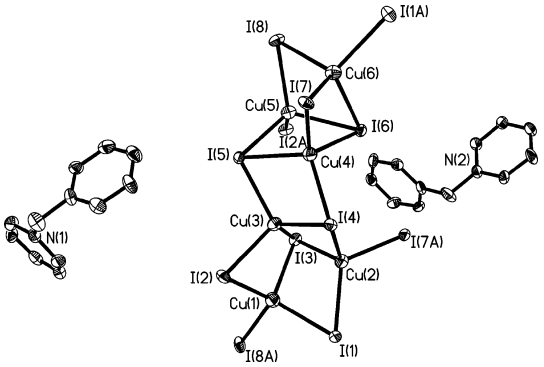

Figure 1. Asymmetric unit diagram of **1**.

Cu interactions. Cu(1), Cu(2), and Cu(3) or Cu(4), Cu(5) and Cu(6)I_4 tetrahedral share edges to form an incomplete cubane-like Cu_3I_7 SBU A(B) (Figure 1). One A(B) links three neighboring B(A) leading to a propellane-like chiral AB_3 (BA_3) motif with C_3 symmetry[9] (Figure 2a). Further connection gives rise to a three-dimensional (3D) open framework with (10,3)-a net (Figure 2b), one of the typical networks for chiral spontaneous resolution, mainly reported in coordination polymers[24] and $[M(ox)_3]^{(6-m)-}$.[25] The V-shaped *N*-Bz-Py^+ are occluded in 3D channels with dihedral angles of 74.288(432) and 87.141(471)°. There exist intermolecular offset $\pi\cdots\pi$ interactions between phenyl and pyridyl ring of adjacent molecules with centroid-to-centroid distances of 3.8512(2), 3.7912(2), and 4.1374(2) Å, respectively, assembling into a 3D (10,3)-a cationic supramolecular net with each cation as a 3-connected node (Figure 2b,c). This complementary relationship with the inorganic framework exhibits excellent symmetrical correlation.

{[N-Bz-Py]$_4$[Ag$_9$I$_{13}$]}$_n$ (**2**). Compound **2** crystallizes in acentric space group *Cc*. The asymmetric unit of compound **2** contains nine Ag(I) atoms and 13 iodine atoms together with four *N*-Bz-Py^+ cations (Figure 3). The Ag–I bond distances range from

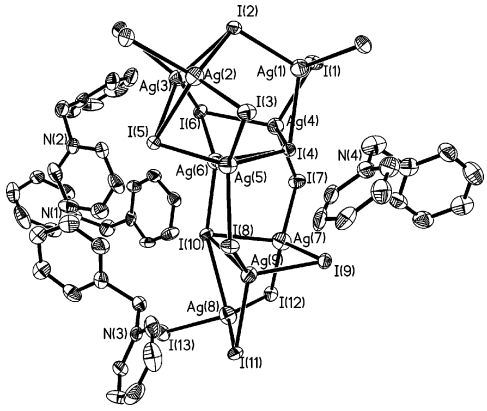

Figure 3. Asymmetric unit diagram of **2**.

2.7753(8) to 3.2376(8) Å, and I–Ag–I bond angles vary between 96.71(2) and 137.49(3), deviating slightly from an ideal tetrahedron except for seriously distorted Ag(8)I_4 tetrahedron with long Ag(8)–I(10) length (3.2376(8) Å). The Ag···Ag distances are in the range of 3.0332(9)–3.4545(9) Å. Except for Ag(7)–Ag(9) (3.4545(9) Å), there exist argentophilic interactions, which are longer than that of

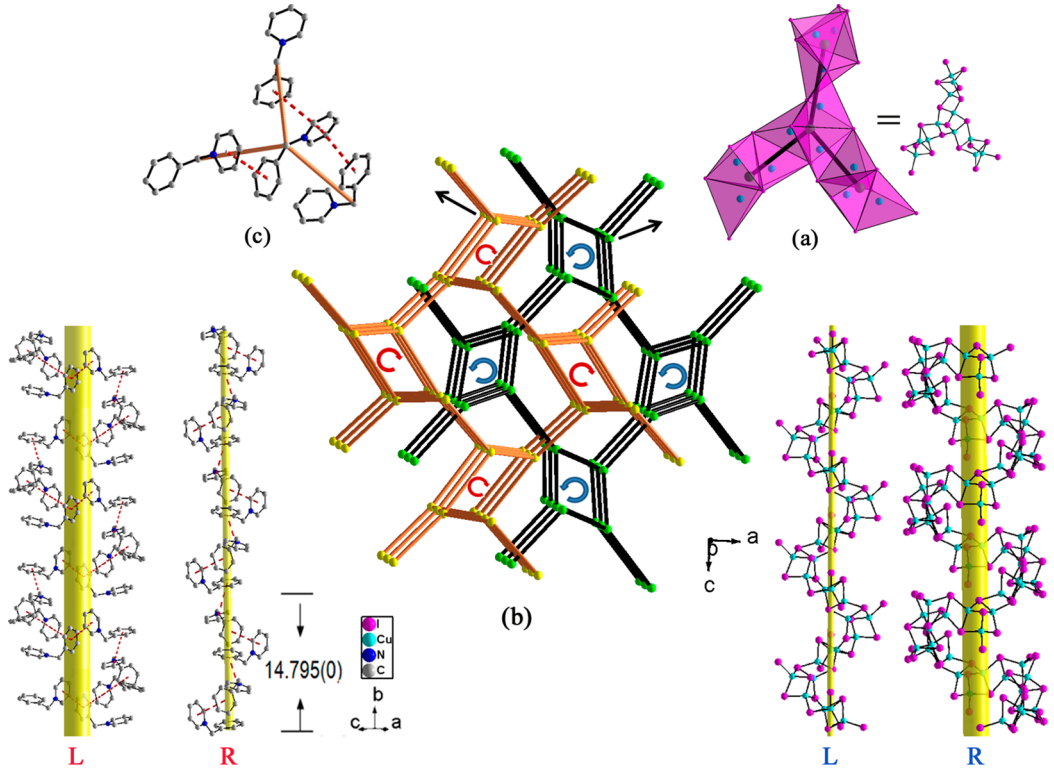

Figure 2. 3-connnected chiral inorganic motif (a), 3-connnected organic subunits via $\pi\cdots\pi$ interactions (c), and interpenetrated anionic–cationic (10,3)-a networks with opposite handedness formed from 1D small and giant helices (b) in **1**. The 3-connected Cu_3I_7 SBU and its connections are represented as green spheres and black straight lines, respectively. The 3-connected organic subunits and its connections are represented by yellow spheres and orange straight lines, respectively.

DOI: 10.1021/acs.inorgchem.5b01331
Inorg. Chem. 2015, 54, 8705–8710

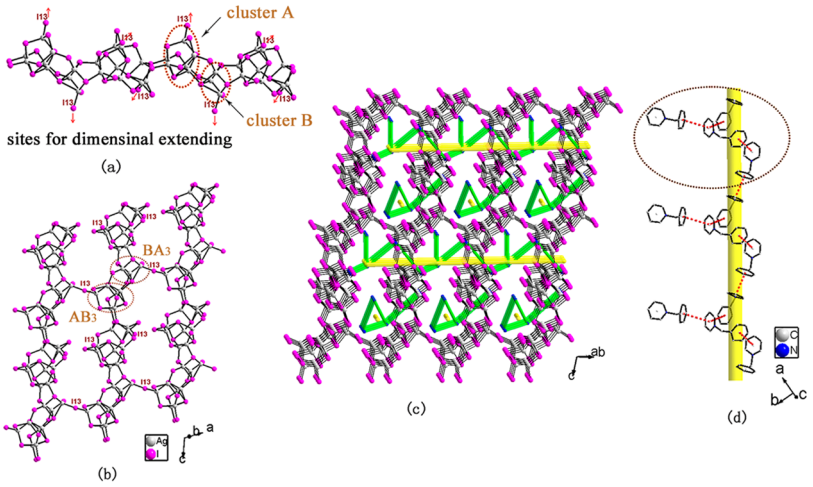

Figure 4. (a) 1D inorganic chain asymmetric connected by Ag_6I_{12} (A) and Ag_3I_7 (B) SBU of **2**. (b) 2D layer via further asymmetric connection between adjacent chains, showing acentric AB_3 (BA_3) motifs of **2**; (c) the cationic supramolecular chains extend along the inorganic channels (the *N*-Bz-Py$^+$, its connection and quasi-helicoidal axes are represented as blue spheres, green straight lines, and yellow stick, respectively). (d) A cationic supramolecular chain with 3-connected units of **2**.

metallic silver (2.88 Å) but shorter than the van der Waals radius sum of silver (3.44 Å). The 3D inorganic framework of **2** is built from the alternatively acentric connections between Ag_6I_{12} SBU (cluster A) and incomplete cubane-like Ag_3I_7 SBU (cluster B) similar to the Cu_3I_7 SBU in **1** (Figure 4). In detail, each A(B) is linked with three adjacent B(A) forming acentric AB_3 (BA_3) inorganic motifs, further forming a 3D acentric iodoargentate with an open framework filled by *N*-Bz-Py$^+$ cations (Figure 4b,c). The dihedral angles of V-shaped *N*-Bz-Py$^+$ are 61.156(225), 74.452(257), 79.680(213), and 82.797(235)°, respectively. Connected by offset $\pi\cdots\pi$ stacking interactions (centroid-to-centroid distances: d_1 = 3.7730(2), d_2 = 3.9696(2), d_3 = 3.6199(1), and d_4 = 4.0260(2) Å), *N*-Bz-Py$^+$ assemble into a supramolecular quasi-threefold helical chain with external appended *N*-Bz-Py$^+$ in a unilateral manner and 3-connected units similar to **1** (Figure 4d).

3.3. Influences of *N*-Bz-Py$^+$ Cation on the Assembly of Noncentrosymmetric Hybrids. Cationic supramolecular aggregates have recently been demonstrated as actual and active structure-directing entities.[26] Compared with dipyridiniomethane in $[C_{11}H_{12}N_2]_2[Cu_2I_6]$,[27] *N*-Bz-Py$^+$ cationic unique spatial and electronic configuration and consequent supramolecular assembly of *N*-Bz-Py$^+$ cations realize the amplification and transfer of asymmetric information and finally direct the construction of two NCS iodometallates. In contrast to chiral templates associated with configuration,[8−12] chiral SDAs associated with conformation such as *N*-Bz-Py$^+$ were rarely reported in the directed synthesis of NCS materials. Furthermore, remarkable structural differences reveal distinct crystallizing habits[28] of inorganic components, which also witness unique NCS supramolecular assembly and diverse structural matching abilities of *N*-Bz-Py$^+$. Until now, most of the reported ionic solids with homochiral (10,3)-a net were metal oxalates with ready-made chiral metallic centers, while templates only provide a chance for the chiral spontaneous resolution of $[M(ox)_3]^{(6-m)-}$ due to their appropriate symmetry (D_3), charge, and size, such as tris-chelated transition-metal complexes,[25c] supramolecular cations Ph_3MeP^+ [25a] and $\{(Me_2NH_2)_6SO_4\}^{4+}$.[25b] However, *N*-Bz-Py$^+$ cationic aggregates with homochiral (10,3)-a net in **1** and acentric supramolecular chains in **2** present rare and interesting examples due to their active charge, spatial and symmetrical directing effects on the assembly of achiral inorganic building units.

3.4. Thermogravimetric Analyses. The thermal decomposition behavior of **1** and **2** are exhibited in Figure S3. Two compounds are thermally stable to 235 °C. They exhibit two stages of weight losses in **1** and three stages in **2**. The first stage occurs in the range of 235−499 °C in **1** and 234−455 °C in **2**, probably corresponding to the loss of *N*-Bz-Py$^+$I$^-$ (Calcd: 34.03%; Found: 30.27% for **1**, Calcd: 35.98%; Found: 28.32% for **2**). A slightly different temperature of **1** and **2** may be attributed to the difference of the local environments and weak interactions of cations.[29] The weight loss in the range of 499−572 °C for **1** and 534−800 and 800−900 °C for **2** is assigned to the decomposition of iodometallate frameworks. Calcination for **1** at 600 °C, for **2** at 900 °C, and further ICP analysis indicate 79.82 wt % of Cu for **1** and 99.96 wt % of Ag for **2**, which are consistent with the assignment of CuO for **1** and metal Ag for **2** (calculated: 79.87 and 100.00 wt %) and percentage of residues CuO or Ag (Calcd: 27.54%; Found: 29.98% for **1**, Calcd: 29.36%; Found: 31.14% for **2**).

3.5. Second Harmonic Generation Measurement. As shown in Figure 5, SHG measurements are type-I phase-

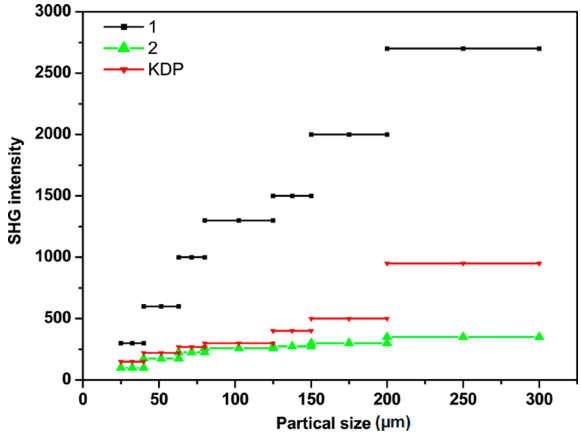

Figure 5. Phase-matching curves, that is, particle size vs SHG intensity of **1** and **2** at the wavelengths of 532 nm with KDP as a reference.

DOI: 10.1021/acs.inorgchem.5b01331
Inorg. Chem. 2015, 54, 8705−8710

matchable in UV regions by examining the effect of the sample size on the SHG intensity.[30] Their SHG responses (~2.8 times and 0.4 times that of KDP for **1** and **2**) reveal obvious chirality or acentricity, which are additionally affected by possible intermolecular charge separation between anionic framework and pyridinium cations.[24c] The SHG response of **1** is much stronger than that of **2**, which is probably due to the difference in structure and transition moment of inorganic framework, which may need further verification. However, compared with a good donor−acceptor chromophore such as stilbazolium cations,[1a,3a,31] **1** and **2** show such slightly weaker responses. Air-stable, insoluble in most solvents, and thermal stabilities imply that two compounds may be a potential candidate for second-order NLO materials.

3.6. Optical Absorption Spectra and Thermochromic Property. The experimental XRPD pattern of **1** and **2** agrees with the simulated one (Figure S4), proving that the as-synthesized products are a single phase. The UV−vis diffuse reflectance spectra of **1** and **2** were measured at room temperature and at 77 K (Figure 6). The absorption (a/S)

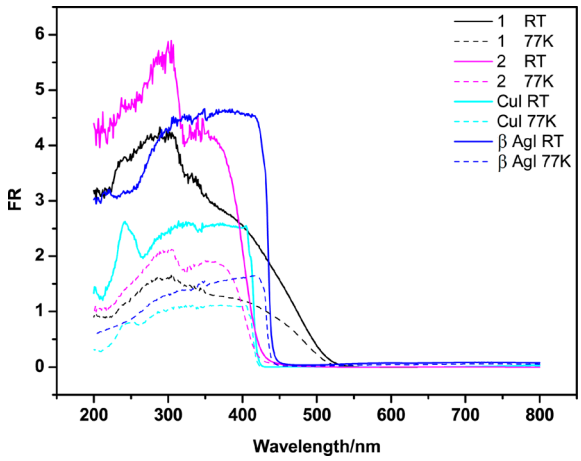

Figure 6. UV−vis diffuse reflectance spectrum for **1**, **2**, and CuI at room temperature (RT) and at 77 K.

data were calculated on the reflectance data with the Kubelka−Munk function. The band gaps (2.52 eV for **1** and 3.02 eV for **2**) were evaluated with the straightforward extrapolation method[32] based on Figure S5, suggesting a semiconductive nature. Noteworthy, **1** exhibits 0.43 eV red shift with respect to that of CuI (2.95 eV), and **2** is 0.21 eV blue-shifted compared with bulk β-AgI (2.81 eV), revealing obvious intermolecular charge transfer (CT) effect[21,22c] in **1**, which is probably due to the strong donating ability of iodocuprate framework, rich $\pi-\pi$ interactions,[26f] and consequent packing modes.

As presented in Figure 7, compound **1** could change color from orange (room temperature, RT) to yellow (liquid nitrogen, 77 K) and gradually return to the initial color with the temperature recovery. The comparisons of the single-crystal data, XRPD patterns at RT and at 100 K (Table 1, Table S1, and Figure S4) and UV−vis absorption spectra at RT and at 77 K (Figure 6) indicate no obvious structural change and shift of absorption edge, which imply no phase change or association/dissociation of CT complexes and effect of lattice contraction at low temperature.[33] Different from the uniformly decrease of absorption intensity for CuI, remarkably different decrease of absorption from 400 to 530 nm is in good agreement with the thermochromism of **1**, which can be attributed to the

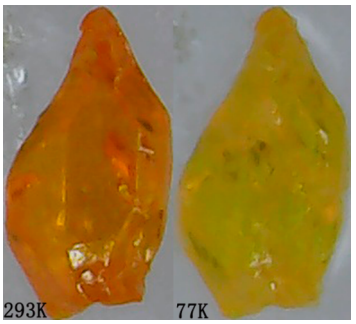

Figure 7. Thermochromic behavior of **1**: Digital photograph of a crystal taken at room temperature (293 K) and temperature of liquid nitrogen (77 K).

temperature effect directly on the population of intermolecular CT rather than on structural variations.[21,26f] Although iodoargentate hybrids based on CT have been found in our previous work,[21,26f] no thermochromic iodocuprate was documented until now.

4. CONCLUSION

In summary, synthesis and characterization of two NCS 3D iodides of d^{10} cation (Cu^+, Ag^+) hybrids present that judicious choice of chiral SDAs and supramolecular assembly via multiple noncovalent interactions can be used as an effective route for the symmetrically related construction of NCS materials. Furthermore, the hybridization of electronic-rich iodometallates and electronic-deficient aromatic cations would be beneficial to the research and development of multifunctional materials.

■ ASSOCIATED CONTENT

Supporting Information

The Supporting Information is available free of charge on the ACS Publications website at DOI: 10.1021/acs.inorgchem.5b01331.

Oscilloscope traces of the SHG signals of **1**, **2**, and KDP at the same particle size of 200−300 μm, infrared spectroscopy, thermogravimetric analyses, XRPD patterns, optical absorption spectra at ambient temperature and at 77 K, and selected bond lengths (Å) and angles (deg) for **1** and **2**. (PDF)

X-ray crystallographic information for compound **1** at 293 K. (structure factors CIF)

X-ray crystallographic information for compound **2** at 293 K. (structure factorsCIF)

X-ray crystallographic information for compounds (CIF)

X-ray crystallographic information for compound **1** at 100 K (structure factors CIF)

■ AUTHOR INFORMATION

Corresponding Author

*Fax & Phone: Int. code +86 (0) 357 2053716. E-mail: yunlongfu@dns.sxnu.edu.cn.

Notes

The authors declare no competing financial interest.

■ ACKNOWLEDGMENTS

This work is supported by the National Natural Science Foundation of China (no. 21171110) and the Specialized

DOI: 10.1021/acs.inorgchem.5b01331
Inorg. Chem. 2015, 54, 8705−8710

Research Fund for the Doctoral Program of Higher Education of China (no. 20131404110001).

REFERENCES

(1) (a) Guloy, A. M.; Tang, Z. J.; Miranda, P. B.; Srdanov, V. I. *Adv. Mater.* **2001**, *13*, 833−835. (b) Cariati, E.; Macchi, R.; Roberto, D.; Ugo, R.; Galli, S.; Casati, N.; Macchi, P.; Sironi, A.; Bogani, L.; Caneschi, A.; Gatteschi. *J. Am. Chem. Soc.* **2007**, *129*, 9410−9420.

(2) (a) Chang, H. Y.; Kim, S. H.; Halasyamani, P. S.; Ok, K. M. *J. Am. Chem. Soc.* **2009**, *131*, 2426−2427. (b) Chang, H. Y.; Kim, S. H.; Ok, K. M.; Halasyamani, P. S. *Chem. Mater.* **2009**, *21*, 1654−1662.

(3) (a) Xu, G.; Li, Y.; Zhou, W. W.; Wang, G. J.; Long, X. F.; Cai, L. Z.; Wang, M. S.; Guo, G. C.; Huang, J. S.; Bator, G.; Jakubas, R. *J. Mater. Chem.* **2009**, *19*, 2179−2183. (b) Zhao, H. R.; Li, D. P.; Ren, X. M.; Song, Y.; Jin, W. Q. *J. Am. Chem. Soc.* **2010**, *132*, 18−19. (c) Guo, Z.; Cao, R.; Wang, X.; Li, H.; Yuan, W.; Wang, G.; Wu, H.; Li, J. *J. Am. Chem. Soc.* **2009**, *131*, 6894−6895.

(4) Choi, M. H.; Kim, S. H.; Chang, H. Y.; Halasyamani, P. S.; Ok, K. M. *Inorg. Chem.* **2009**, *48*, 8376−8382.

(5) (a) Treacy, M. M. J.; Newsam, J. M. *Nature* **1988**, *332*, 249−251. (b) Ma, L. Q.; Abney, C.; Lin, W. B. *Chem. Soc. Rev.* **2009**, *38*, 1248−1256.

(6) Morris, R. E.; Bu, X. H. *Nat. Chem.* **2010**, *2*, 353−361.

(7) Li, M. R.; Liu, W.; Ge, M. H.; Chen, H. H.; Yang, X. X.; Zhao, J. T. *Chem. Commun.* **2004**, 1272−1273.

(8) (a) Lin, H. M.; Lii, K. H. *Inorg. Chem.* **1998**, *37*, 4220−4222. (b) Lin, C. H.; Wang, S. L. *Inorg. Chem.* **2001**, *40*, 2918−2921.

(9) (a) Williams, D. J.; Kruger, J. S.; McLeroy, A. F.; Wilkinson, A. P.; Hanson, J. C. *Chem. Mater.* **1999**, *11*, 2241−2249. (b) Stalder, S. M.; Wilkinson, A. P. *Chem. Mater.* **1997**, *9*, 2168−2173. (c) Gray, M. J.; Jasper, J. D.; Wilkinson, A. P.; Hanson, J. C. *Chem. Mater.* **1997**, *9*, 976−980. (d) Wang, Y.; Chen, P.; Li, J. Y.; Yu, J. H.; Xu, J.; Pan, Q. H.; Xu, R. R. *Inorg. Chem.* **2006**, *45*, 4764−4766. (e) Chen, P.; Li, J. Y.; Duan, F. Z.; Yu, J. H.; Xu, R. R.; Sharma, R. P. *Inorg. Chem.* **2007**, *46*, 6683−6687. (f) Wang, Y.; Yu, J. H.; Guo, M.; Xu, R. R. *Angew. Chem., Int. Ed.* **2003**, *42*, 4089−4092.

(10) (a) Yu, J. H.; Xu, R. R. *J. Mater. Chem.* **2008**, *18*, 4021−4030. (b) Wang, Y.; Yu, J. H.; Li, Y.; Shi, Z.; Xu, R. R. *Chem. - Eur. J.* **2003**, *9*, 5048−5055.

(11) (a) Zhang, H. X.; Zhang, J.; Zheng, S. T.; Yang, G. Y. *Inorg. Chem.* **2003**, *42*, 6595−6597. (b) Yang, G.; Sevov, S. C. *Inorg. Chem.* **2001**, *40*, 2214−2215. (c) Lin, Z. E.; Zhang, J.; Zhao, J. T.; Zheng, S. T.; Pan, C. Y.; Wang, G. M.; Yang, G. Y. *Angew. Chem., Int. Ed.* **2005**, *44*, 6881−6884.

(12) Zhou, J.; Zheng, S. T.; Zhang, M. Y.; Liu, G. Z.; Yang, G. Y. *CrystEngComm* **2009**, *11*, 2597−2600.

(13) Ayyappan, S.; Bu, X.; Cheetham, A. K.; Rao, C. N. R. *Chem. Mater.* **1998**, *10*, 3308−3310.

(14) Kim, J. H.; Baek, J.; Halasyamani, P. S. *Chem. Mater.* **2007**, *19*, 5637−5641.

(15) Guo, D. W.; Yao, S. Y.; Zhang, G.; Tian, Y. Q. *CrystEngComm* **2010**, *12*, 2989−2995.

(16) Guo, Y. H.; Shi, Z.; Yu, J. H.; Wang, J. D.; Liu, Y. L.; Bai, N.; Pang, W. Q. *Chem. Mater.* **2001**, *13*, 203−207.

(17) (a) Lawton, S. L.; Rohrbaugh, W. J. *Science* **1990**, *247*, 1319−1322. (b) Férey, G. *Chem. Mater.* **2001**, *13*, 3084−3098. (c) Li, H. H.; Xing, Y. Y.; Lian, Z. X.; Gong, A. W.; Wu, H. Y.; Li, Y.; Chen, Z. R. *CrystEngComm* **2013**, *15*, 1721−1728.

(18) (a) Yu, T. L.; An, L.; Zhang, L.; Shen, J. J.; Fu, Y. B.; Fu, Y. L. *Cryst. Growth Des.* **2014**, *14*, 3875−3879. (b) Shen, J. J.; Zhang, C. F.; Yu, T. L.; An, L.; Fu, Y. L. *Cryst. Growth Des.* **2014**, *14*, 6337−6342.

(19) (a) Hou, J. J.; Guo, C. H.; Zhang, X. M. *Inorg. Chim. Acta* **2006**, *359*, 3991−3995. (b) Chen, Y.; Yang, Z.; Guo, C. X.; Ni, C. Y.; Ren, Z. G.; Li, H. X.; Lang, J. P. *Eur. J. Inorg. Chem.* **2010**, *2010*, 5326−5333. (c) Chan, H.; Chen, Y.; Dai, M.; Lü, C. N.; Wang, H. F.; Ren, Z. G.; Huang, Z. J.; Ni, C. Y.; Lang, J. P. *CrystEngComm* **2012**, *14*, 466−473. (d) Hou, J. J.; Li, S. L.; Li, C. R.; Zhang, X. M. *Dalton Trans.* **2010**, *39*, 2701−2707.

(20) (a) *CrysAlisPro,* version 1.171.33.56; Oxford Diffraction Ltd: Oxfordshire, U.K., 2010.

(21) (a) Sheldrick, G. M. *Acta Crystallogr., Sect. A: Found. Crystallogr.* **2008**, *A64*, 112−122. (b) Sheldrick, G. M. *SHELXS-97,* A Program for X-ray Crystal Structure Solution, and *SHELXL-97,* A Program for X-ray Structure Refinement; Göttingen University: Germany, 1997.

(22) Kurtz, S. K.; Perry, T. T. *J. Appl. Phys.* **1968**, *39*, 3798−3813.

(23) Khili, H.; Chaari, N.; Fliyou, M.; Koumina, A.; Chaabouni, S. *Polyhedron* **2012**, *36*, 30−37.

(24) (a) Decurtins, S.; Schmalle, H. W.; Pellaux, R.; Schneuwly, P.; Hauser, A. *Inorg. Chem.* **1996**, *35*, 1451−1460. (b) Bu, X. H.; Chen, W.; Du, M.; Biradha, K.; Wang, W. Z.; Zhang, R. H. *Inorg. Chem.* **2002**, *41*, 437−439. (c) Liu, Q. Y.; Wang, Y. L.; Zhang, N.; Jiang, Y. L.; Wei, J. J.; Luo, F. *Cryst. Growth Des.* **2011**, *11*, 3717−3720. (d) Han, L. L.; Zhang, X. Y.; Chen, J. S.; Li, Z. H.; Sun, D. F.; Wang, X. P.; Sun, D. *Cryst. Growth Des.* **2014**, *14*, 2230−2239.

(25) (a) Russell, V. M.; Craig, D. C.; Scudder, M. L.; Dance, I. G. *CrystEngComm* **2001**, *2*, 96−106. (b) Li, C. R.; Li, S. L.; Zhang, X. M. *Cryst. Growth Des.* **2009**, *9*, 1702−1707. (c) Pointillart, F.; Train, C.; Gruselle, M.; Villain, F.; Schmalle, H. W.; Talbot, D.; Gredin, P.; Decurtins, S.; Verdaguer, M. *Chem. Mater.* **2004**, *16*, 832−841.

(26) (a) Gómez-Hortigüela, L.; García, R.; López-Arbeloa, F.; Corà, F.; Pérez-Pariente, J. *J. Phys. Chem. C* **2010**, *114*, 8320−8327. (b) Álvaro-Muñoz, T.; López-Arbeloa, F.; Pérez-Pariente, J.; Gómez-Hortigüela, L. *J. Phys. Chem. C* **2014**, *118*, 3069−3077. (c) Corma, A.; Rey, F.; Rius, J.; Sabater, M. J.; Valencia, S. *Nature* **2004**, *431*, 287−290. (d) Martínez-Franco, R.; Cantín, Á.; Moliner, M.; Corma, A. *Chem. Mater.* **2014**, *26*, 4346−4353. (e) Zhang, Z. J.; Guo, G. C.; Xu, G.; Fu, M. L.; Zou, J. P.; Huang, J. S. *Inorg. Chem.* **2006**, *45*, 10028−10030. (f) Yu, T. L.; Shen, J. J.; Wang, Y. L.; Fu, Y. L. *Eur. J. Inorg. Chem.* **2015**, *2015*, 1989−1996. (g) Wiebcke, M.; Bögershausen, A.; Koller, H. *Microporous Mesoporous Mater.* **2005**, *78*, 97−102.

(27) Hartl, H.; Brudgam, I.; Mahdjour-Hassan-Abadi, F. *Z. Naturforsch., B: J. Chem. Sci.* **1985**, *40*, 1032.

(28) Niu, Y. Y.; Song, Y. L.; Zhang, N.; Hou, H. W.; Che, D. J.; Fan, Y. T.; Zhu, Y.; Duan, C. Y. *Eur. J. Inorg. Chem.* **2006**, *2006*, 2259−2267.

(29) Zhang, W. L.; Huang, Z. P.; Ma, C. J.; Zai, Y. X.; Yang, Q.; Niu, Y. Y. *Inorg. Chim. Acta* **2015**, *425*, 52−60.

(30) (a) Kurtz, S. K.; Perry, T. T. *J. Appl. Phys.* **1968**, *39*, 3798−3813. (b) Song, J. L.; Hu, C.-L.; Xu, X.; Kong, F.; Mao, J. G. *Inorg. Chem.* **2013**, *52*, 8979−8986. (c) Li, L.; Ma, J. X.; Song, C.; Chen, T. L.; Sun, Z. H.; Wang, S. Y.; Luo, J. H.; Hong, M. C. *Inorg. Chem.* **2012**, *51*, 2438−2442.

(31) (a) Cariati, E.; Ugo, R.; Cariati, F.; Roberto, D.; Masciocchi, N.; Galli, S.; Sironi, A. *Adv. Mater.* **2001**, *13*, 1665−1668. (b) Cariati, E.; Macchi, R.; Roberto, D.; Ugo, R.; Galli, S.; Masciocchi, N.; Sironi, A. *Chem. Mater.* **2007**, *19*, 3704−3711.

(32) (a) Wendlandtand, W. W.; Hecht, H. G. *Reflectance Spectroscopy;* Interscience Publishers: New York, 1966. (b) Schevciw, O.; White, W. B. *Mater. Res. Bull.* **1983**, *18*, 1059−1068.

(33) (a) Lemmerer, A.; Billing, D. G. *Dalton Trans.* **2012**, *41*, 1146−1157. (b) Haristoy, D.; Tsiourvas, D. *Chem. Mater.* **2003**, *15*, 2079−2083. (c) Goforth, A. M.; Tershansy, M. A.; Smith, M. D.; Peterson, L., Jr.; Kelley, J. G.; DeBenedetti, W. J. I.; zur Loye, H. C. *J. Am. Chem. Soc.* **2011**, *133*, 603−612. (d) Lemmerer, A.; Billing, D. G. *Dalton Trans.* **2012**, *41*, 1146−1157. (e) Burns, M. C.; Tershansy, M. A.; Ellsworth, J. M.; Khaliq, Z.; Peterson, L., Jr.; Smith, M. D.; zur Loye, H. C. *Inorg. Chem.* **2006**, *45*, 10437−10439. (f) Guo, H. X.; Zhang, Y.; Li, X. Z.; Weng, W. *Inorg. Chem. Commun.* **2010**, *13*, 425−428.

DOI: 10.1021/acs.inorgchem.5b01331
Inorg. Chem. 2015, 54, 8705−8710